http://www.kidney-international.org

Renal L-type fatty acid-binding protein mediates the bezafibrate reduction of cisplatin-induced acute kidney injury

K Negishi[1], E Noiri[1,2], R Maeda[1,2], D Portilla[3], T Sugaya[4] and T Fujita[1]

[1]*Department of Nephrology and Endocrinology, Hemodialysis and Apheresis, University Hospital, University of Tokyo, Tokyo, Japan;* [2]*Center of NanoBio Integration, University of Tokyo, Tokyo, Japan;* [3]*Division of Nephrology, Department of Medicine, University of Arkansas for Medical Sciences and Central Arkansas Veterans Healthcare Systems, Little Rock, Arkansas, USA and* [4]*Center for Developmental Biology, RIKEN, Kobe, Japan*

Fibrates, the PPARα ligand-like compounds increase the expression of proximal tubule liver fatty acid binding protein (L-FABP) and significantly decrease cisplatin-induced acute kidney injury. To study whether the bezafibrate-mediated upregulation of renal L-FABP was involved in this cytoprotective effect we treated transgenic mice of PPAR agonists inducible human L-FABP expression with cisplatin in the presence or absence of bezafibrate. Blood urea nitrogen was unchanged in the first day but increased 3 days after cisplatin. While urinary L-FABP increased over 100-fold 1 day after cisplatin treatment in the transgenic mice it was significantly reduced when these transgenic mice were pretreated with bezafibrate. Cisplatin-induced renal necrosis and apoptosis were significantly reduced in bezafibrate pretreated transgenic mice and this correlated with decreased accumulation of lipid and lipid peroxidation products. Immunohistochemical analysis of kidney tissue of bezafibrate-cisplatin-treated transgenic mice showed preservation of cytoplasmic L-FABP in the proximal tubule, but this was reduced in transgenic mice treated only with cisplatin. L-FABP mRNA and protein levels were significantly increased in bezafibrate-cisplatin-treated transgenic mice when compared to mice not fibrate treated. Our study shows that the bezafibrate-mediated upregulation of proximal tubule L-FABP plays a pivotal role in the reduction of cisplatin-induced acute kidney injury.

Kidney International (2008) **73,** 1374–1384; doi:10.1038/ki.2008.106; published online 26 March 2008

KEYWORDS: acute renal failure; fibrate; PPAR-α; apoptosis; lipotoxicity; biomarker; humanized mice

Correspondence: *E Noiri, Department of Nephrology, 107 Lab., University Hospital, University of Tokyo, 7-3-1 Hongo, Bunkyo, Tokyo 113-8655, Japan. E-mail: noiri-tky@umin.ac.jp*

Received 15 September 2007; revised 3 December 2007; accepted 30 January 2008; published online 26 March 2008

The intracellular fatty acid-binding proteins (FABPs) belong to a superfamily of lipid-binding proteins with low molecular weight (14–15 kDa), which are classified according to their predominant tissue localization. Nine different FABPs have been reported with tissue-specific distribution that includes L (liver), I (intestinal), H (muscle and heart), A (adipocyte), E (epidermal), Il (ileal), B (brain), M (myelin), and T (testis).[1] All FABPs bind to long-chain fatty acids. However, binding affinity and ligand selectivity are different for each isoform.[2] The L-type of FABP (L-FABP) is highly expressed in hepatocytes, where it represents 5% of the total cytosolic protein. In the human kidney, L-FABP is predominantly expressed in proximal tubules. L-FABP facilitates the cellular uptake, transport, and metabolism of fatty acids, and it is also involved in the regulation of gene expression and cell differentiation.[3–5] A previous report demonstrated that 4-hydroxy-nonenal, a cytotoxic α,β-unsaturated acyl aldehyde resulting from lipid peroxidation in response to oxidative stress, was able to bind E-FABP.[6] Similarly, Wang *et al.*[7] showed *in vitro* the protective role of L-FABP in reducing oxidative stress in hypoxia–reoxygenation. More recently, Yamamoto *et al.*[8] demonstrated that urinary L-FABP behaved as a sensitive biomarker in response to ischemic stress in human kidney transplantation. In addition, they show that human transgenic (Tg) L-FABP mice have less tubular injury during ischemia–reperfusion and intracellular oxidative stress.[8] These studies suggest that L-FABP not only participates in fatty acid trafficking but also serves as an early indicator of ischemic conditions and as a crucial cellular antioxidant molecule.

Recent work also suggests that L-FABP is a member of the lipocalin superfamily, which under normal conditions resides in the lysosomal compartment of the proximal tubule, but can also be reabsorbed from the glomerular filtrate via megalin, a multiligand proximal tubule endocytic receptor.[9]

Cisplatin (CP)-induced acute kidney injury (AKI) is a well-studied model of nephrotoxicity in rodents. The most susceptible part of the kidney injured by CP is the S3 segment of the proximal tubule. Tubular damage by CP is dose

dependent. Kidney injury is rather mild when mice receive $<10\,mg\,kg^{-1}$ compared to $>10\,mg\,kg^{-1}$. The mortality rate increases remarkably when mice receive $20\,mg\,kg^{-1}$: renal injury is more extensive, and mice do not survive more than 5 days. Hishikawa *et al.*[10] tried to determine the marginal dosage of CP that shows reasonably severe renal damage and enables survival of more than 4 days, and they concluded that the dose needed was $12.5\,mg\,kg^{-1}$. For this study, $20\,mg\,kg^{-1}$ was used to examine the efficacy of bezafibrate (Bz) to ameliorate lethally induced injury by CP.

Peroxisome proliferator-activated receptors (PPARs) are transcription factors that involve various regulations of lipid and glucose metabolism, adipogenesis, and inflammation.[11] Three different isotypes of PPAR family have been identified: PPAR-α, PPAR-β, and PPAR-γ. All of these isotypes of PPARs are known to reside in the kidney. PPAR-α and PPAR-γ are nuclear receptors that, besides being concerned with the control of fatty acids and glucose metabolism, display anti-inflammatory capabilities.[2] PPAR-α exists in renal proximal tubules and, subsequent to its activation by the ligand, heterodimerizes with retinoic X receptor RXR, and regulates gene transcription by binding to PPAR response elements located in the regulatory regions of target genes. In a previous study, Portilla and co-workers demonstrated that the efficacy of fibrate, a known PPAR-α ligand, administered before AKI, prevented the inhibition of fatty acid oxidation and accumulation of non-esterified fatty acid in renal tissue caused by CP and that it further ameliorated apoptotic and necrotic proximal tubule cell death. That administration resulted in significant protection of renal function only in PPAR-α wild-type (WT) mice and not in PPAR-α null mice.[12–14] Recently, quantitative immunofluorescent analysis revealed that a PPAR-α ligand-like fibrate increases the expression of peroxisomal proteins in mouse kidney tissue. A recent study suggests that increased expression of the proximal tubule L-FABP, using a PPAR-α ligand-like fibrate, ameliorates CP-induced AKI.[15] This study further intends to elucidate the involvement of L-FABP in Bz-induced protection against CP-induced AKI using human L-FABP (hL-FABP) Tg mice.

L-FABP is not normally expressed in mouse kidney tissue unless mice are treated with fibrates; however, higher levels of L-FABP protein expression are found in human proximal tubules.[8,16,17] Therefore, it is difficult to conduct renal *in vivo* experiments using WT mice to examine the role of L-FABP in AKI. For practical purposes, WT mice of the C57BL/6 strain are considered as an example of naturally occurring renal L-FABP-knockout mice. We recently developed hL-FABP Tg mice in which the promoter region of hL-FABP was overexpressed in C57BL/6. Therefore, the distribution of L-FABP was similar to that in humans and suitable for translational research of this protein. In addition, we have developed an enzyme-linked immunosorbent assay system for hL-FABP, which does not cross-react with rodent L-FABP.[18–20] The combination of hL-FABP Tg and hL-FABP enzyme-linked immunosorbent assay has been used as novel tool to examine the role of this biomarker in a wide variety of human renal diseases. The results of this study (1) underscore the protective role of Bz in reducing CP-induced AKI, (2) elucidate the role of renal L-FABP in Bz-mediated cytoprotection, and (3) demonstrate the potential use of urinary hL-FABP in the early diagnosis of CP-mediated AKI.

RESULTS

Time course of CP and fibrate on renal function

Animals were injected with either CP at a dose of 20 mg per kg body weight or saline. Bz was fed for 1 week before CP administration. Blood was drawn serially from each animal up until 72 h after CP administration. Figure 1a presents the dynamics of blood urea nitrogen (BUN). The remarkable increase of BUN found after 48 and 72 h in CP-treated WT mice (61.5 ± 10.5 and 143.4 ± 9.4, respectively; $n = 9$) was not improved using Bz pretreatment in these animals (Bz + CP, 53.4 ± 8.3 and 149.2 ± 12.9, respectively; $n = 9$). Figure 1b depicts the dynamics of BUN in hL-FABP Tg mice. The levels of BUN found after 48 and 72 h in CP-treated Tg mice (58.3 ± 4.0 and 135.5 ± 7.3, respectively; $n = 13$) were equivalent to those of CP-treated WT mice. Renal function estimated as changes in BUN was significantly ameliorated in Bz-pretreated Tg mice (48 h; Bz + CP, 31.7 ± 3.3 and 72 h; 61.6 ± 6.9, respectively; $P < 0.05$, $n = 14$).

Acute tubular damage and apoptosis

Histological analysis of CP-treated WT (Figure 2a), CP-treated Tg (Figure 2b), and WT mice that had been fed Bz (Figure 2c) revealed similar severity of acute tubular damage at 72 h after administration of CP. In addition, CP-treated Tg kidney (72 h after administration) showed the same level of severity of acute tubular damage as did WT

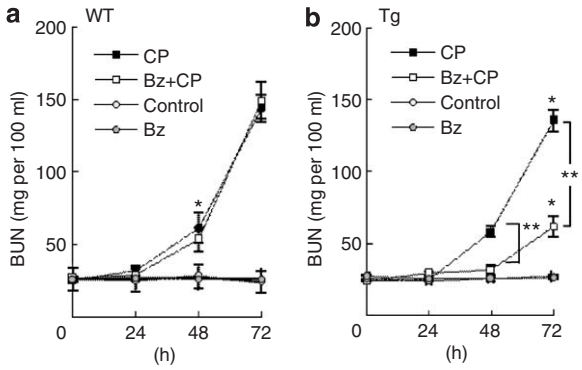

Figure 1 | Time course of BUN. Mice were fed with either a regular diet or a diet containing 0.5% Bz for 7 days before CP administration, as described in Materials and Methods. BUN levels were measured at 24, 48, and 72 h after saline control (control)-, CP (CP)-, Bz + CP (CP pre-fed with Bz)-, and Bz + saline (Bz with saline)-treated mice. Bars correspond to means ± s.e.m. of at least seven independent experiments under each condition. Changes in BUN levels are shown after saline or CP administration in (**a**) WT and (**b**) hL-FABP Tg mice, respectively. Statistically significant differences (*$P < 0.05$, **$P < 0.05$) were indicated when group data were compared to control group data, and when Bz + CP group data were compared to data of the CP-alone group.

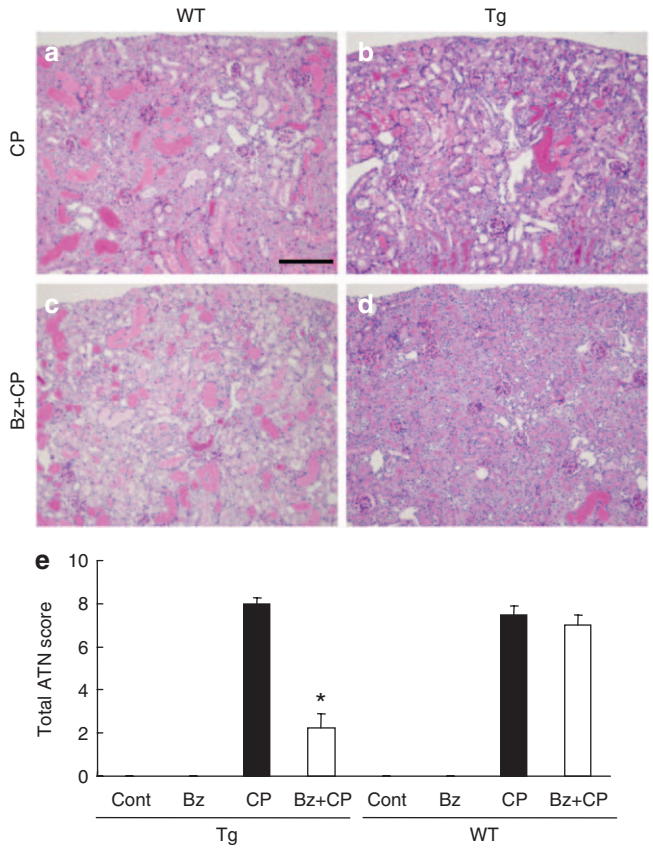

Figure 2 | Morphological analysis of kidney at 72 h after CP administration. The periodic acid-Schiff-stained representative kidney morphology is shown. CP-exposed kidneys were obtained from (**a**) WT and (**b**) Tg mice. Those pretreated with Bz (abbreviated as Bz + CP) were obtained from (**c**) WT and (**d**) Tg mice. Although CP- and Bz + CP-treated WT and CP-treated Tg animals showed severe tubular damage, Bz + CP-treated Tg mice showed remarkable attenuation of tubular damage such as epithelial detachment, dilatation, cast formation, brush-border loss, and the presence of toxic granules (bar = 500 μm). (**e**) Quantitative evaluation of morphologic kidney damage of Tg and WT mice at 72 h after saline or CP administration. ATN scores are expressed as the total of relative severity in each parameter on a scale of 0–2 and represent mean ± s.e.m. of kidney sections from at least seven mice for each experimental condition. Each morphological parameter was scored according to proximal tubule necrosis, brush-border loss, cast formation, tubule dilatation, and tubular degeneration. Statistically significant differences (*$P < 0.05$) were indicated when Bz + CP group data were compared with data of the CP-alone group.

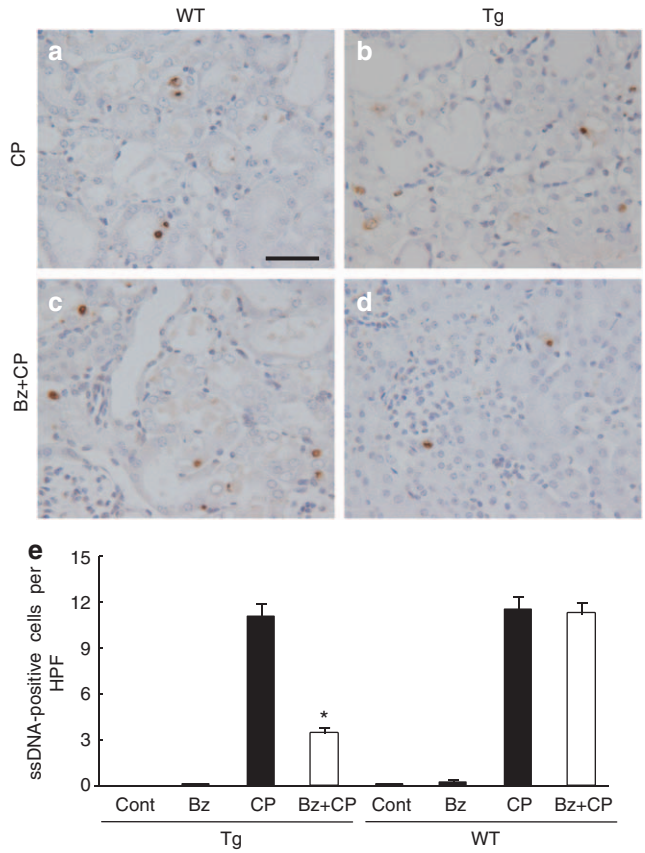

Figure 3 | Apoptosis index by ssDNA staining. The ssDNA-stained representative kidney morphology is shown. CP-exposed kidneys were obtained from (**a**) WT and (**b**) Tg mice. Those pretreated with Bz (abbreviated as Bz + CP) were obtained from (**c**) WT and (**d**) Tg. Bar = 50 μm. (**e**) The apoptosis index was defined as a group average score of ssDNA-positive tubular cells per × 200 visual field taken from five non-overlapping visual fields per mouse. Although the apoptosis index of CP- and Bz + CP-treated WT mice and CP-treated Tg mice at 72 h after CP administration was equally prominent, that of Bz + CP-treated Tg mice was significantly lower than the other groups (*$P < 0.05$).

kidney in terms of tubular dilatation, cast formation, brush-border loss, and detachment of epithelial cells (Figure 2b). In contrast, Bz pretreatment of Tg mice clearly reduced CP-induced acute tubular necrosis (ATN; Figure 2d). ATN scores[21,22] are presented in Figure 2e. No morphological change was found in Bz-treated Tg and WT animals, which were designated as control.

Tubular apoptosis was compared using a well-established early apoptosis indicator, single-stranded DNA (ssDNA) positivity,[23,24] where the tubular cell count per visual field, the apoptosis index, was used for quantitative analyses (Figure 3). The apoptosis index was clearly attenuated in Bz + CP-treated Tg mice, although many ssDNA-positive cells were observed in dilated tubular nuclei and detached tubular cells in Bz + CP-treated WT, CP-treated WT, and CP-treated Tg mice.

Immunohistochemistry of kidney tissue of hL-FABP Tg mice at 72 h after CP or saline administration

No positive immunoreactivity to hL-FABP was found in kidney tissue obtained from WT mice (Figure 4a, d, g, and j). Saline-treated hL-FABP Tg animals showed strong positive staining primarily in the cytoplasm of early (S1 and S2) segments of the proximal tubules and the epithelium of Bowman's capsule (Figure 4c). Moreover, almost all proximal tubular cells showed markedly enhanced positive staining for hL-FABP in Bz-fed Tg mice (Figure 4e and f). Both the Bz- and saline-treated mice showed cytoplasmic dominant enhancement of early segments of the proximal tubules. In Tg kidneys 72 h after CP administration, the nuclear

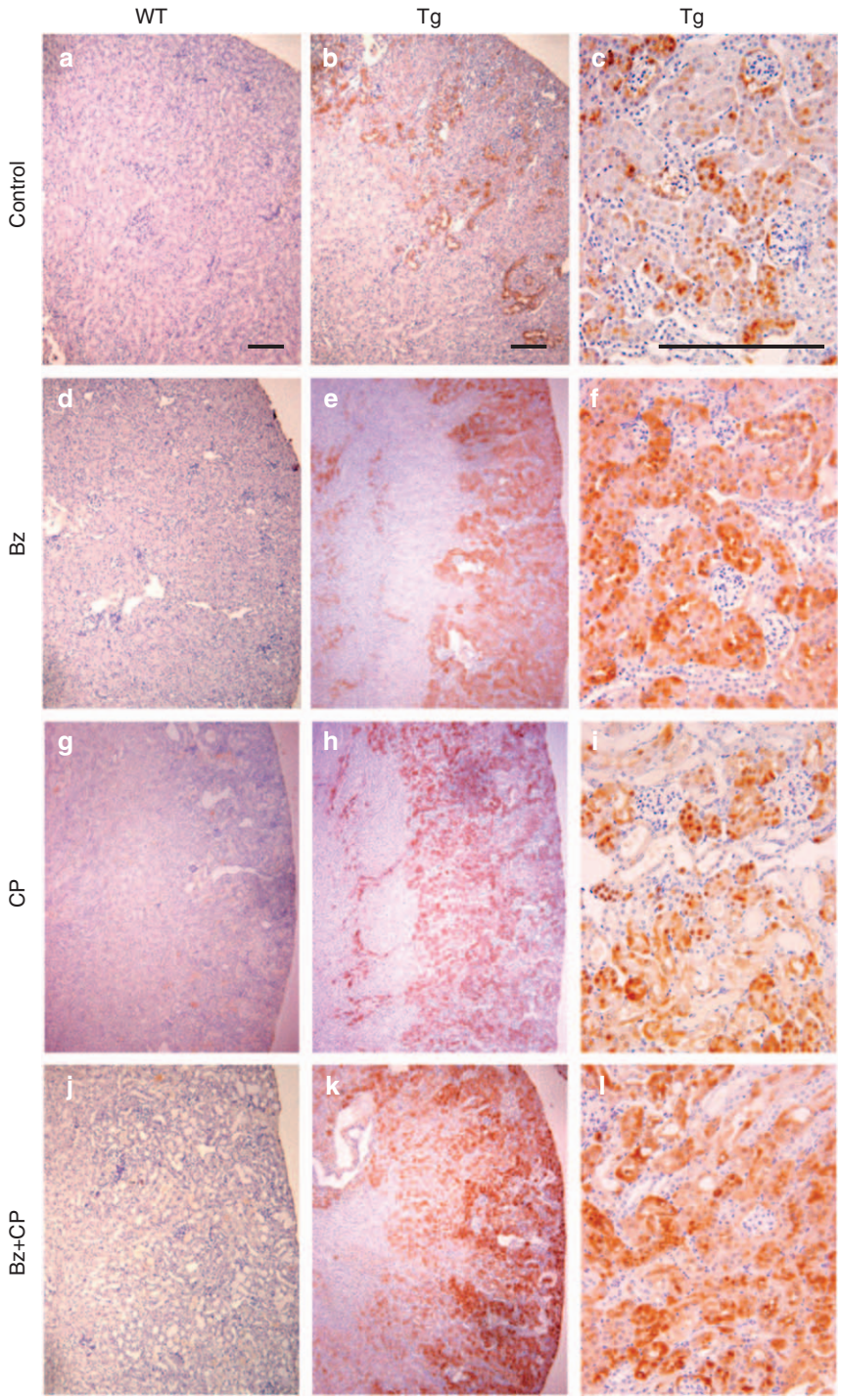

Figure 4 | Immunohistochemistry of hL-FABP staining in kidney at 72 h after CP or saline administration. Middle column demonstrates lower magnification of histology derived from Tg mice. Right column demonstrates those of higher magnification (bar = 250 μm). (**a**, **d**, **g**, **j**) All of WT groups were negative for hL-FABP protein. Compared to (**b**, **c**) control Tg mice kidneys, cytoplasmic staining of hL-FABP in proximal tubules was enhanced in (**e**, **f**) Bz-treated mice kidneys. hL-FABP expression (**h**, **i**) in CP-treated mice kidney was clearly more prominent than the control Tg mice kidney 72 h after CP exposure, but this expression in detached or dilated proximal tubules in (**h**, **i**) CP-treated mice was decreased or absent. (**k**, **l**) The upregulation of hL-FABP was preserved in Bz + CP-treated mice kidney.

dominant pattern of hL-FABP staining was apparent in early segments of proximal tubules and the epithelium of Bowman's capsule (Figure 4i). Some primarily cytoplasmic staining in proximal tubules was also observed in the deep cortex in these CP-treated animals. In the kidneys of CP-treated Tg mice that had been fed Bz, both nuclear staining and cytoplasmic staining were enhanced in the deep cortex as well as in the early segments of proximal tubules (Figure 4k and l). Glomeruli and distal nephron segments were virtually negative. The CP-treated Tg kidneys both with

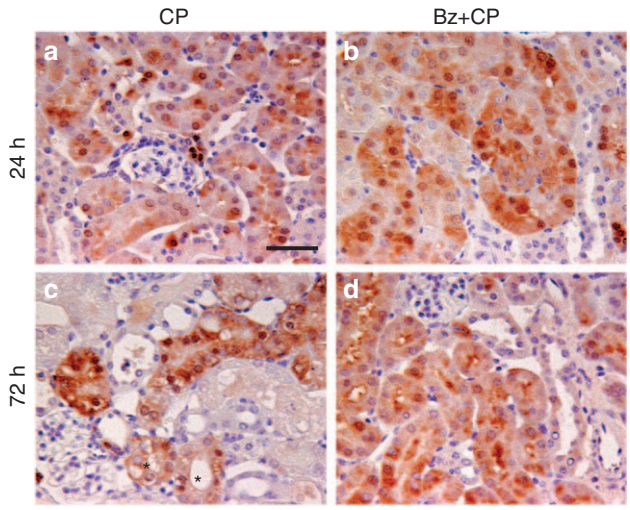

Figure 5 | Immunohistochemistry of hL-FABP staining in Tg mice kidney at 24 and 72 h after CP administration. Representative Tg kidney sections obtained from animals subjected to four experimental conditions: (**a**) CP-treated at 24 h, (**b**) Bz + CP-treated at 24 h, (**c**) CP-treated at 72 h, and (**d**) Bz + CP-treated at 72 h. Those were stained with anti-hL-FABP antibody, as described in Materials and Methods. (**c**) In damaged tubules depicted as asterisks, hL-FABP-positive cells were fewer or non-existent. These findings are thought to indicate that hL-FABP in proximal tubules is not only a stress-responsive protein but also a viability-expressing marker (bar = 50 μm).

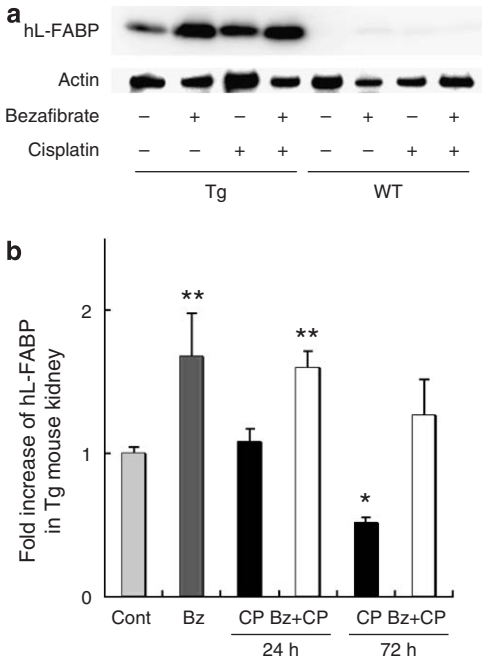

Figure 6 | Western blot analysis of renal hL-FABP protein. (**a**) Representative western blot analysis of hL-FABP. Kidneys were harvested at 72 h after starting experiments. All groups of WT mice were negative. (**b**) Fold increase of renal hL-FABP protein corrected using actin. Statistically significant differences (*$P < 0.05$, **$P < 0.01$) were indicated when the CP -alone group and Bz + CP group were compared, respectively, to the control group.

and without Bz feeding showed almost intact tubules and immunoreactive enhancement of hL-FABP protein when kidneys were immunostained 24 h after CP exposure (Figure 5). In kidneys of CP-treated Tg mice that had been pre-fed with Bz (Figure 5b and d), cytoplasmic dominant patterns in proximal tubular cells were more prominent and stronger than those in CP kidneys (Figure 5a and c). The preservation of proximal tubules 72 h after CP exposure was parallel to the level of tubular expression of hL-FABP protein in both groups (Figure 5c and d). However, the immunoreactivity of hL-FABP was diminished (Figure 5c, asterisks) or undetectable in damaged proximal tubular cells.

Western blot analysis of kidney tissue of hL-FABP Tg mice

Using whole kidney lysate, western blot analysis of hL-FABP protein was performed. Kidneys obtained from Tg mice that had been fed Bz showed significantly higher hL-FABP compared to those in control animals. The Bz + CP-treated Tg mice showed a remarkably higher hL-FABP 24 h after CP administration compared to controls (Figure 6a and b). In contrast, CP-treated Tg mice without Bz 24 h after CP administration showed almost equal expression of hL-FABP compared to controls. Western blot analysis revealed a decrease of hL-FABP expression in CP-AKI, compared to that of 24 h, when kidneys were obtained 72 h after CP exposure. hL-FABP expression remained constant in animals with CP-AKI that had been pre-fed with Bz. No signal existed of hL-FABP in any WT group. These observations are comparable to those related to immunohistochemistry.

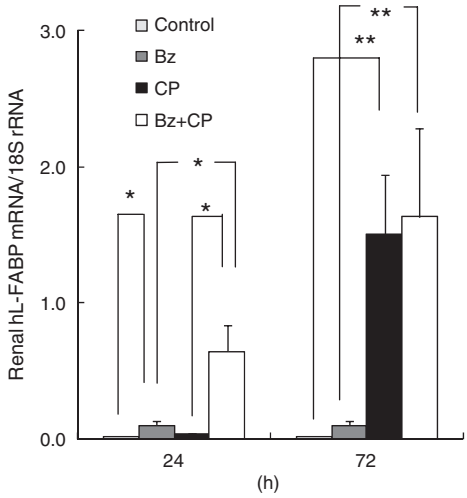

Figure 7 | Quantitative analysis of renal L-FABP mRNA. The fold increase of the renal expression ratio as hL-FABP mRNA/18S rRNA (ribosomal RNA) was quantified using quantitative real-time reverse transcriptase-PCR analysis. Statistically significant differences (*$P < 0.05$, **$P < 0.01$) were indicated when the CP-alone group and Bz + CP group were compared to the control and Bz groups, respectively.

Quantitative real-time reverse transcriptase-PCR analysis of kidney tissue of hL-FABP Tg mice

Figure 7 presents the results of quantitative real-time reverse transcriptase-PCR analysis of renal hL-FABP mRNA

corrected using 18S ribosomal RNA. The Bz-pretreated Tg mice without CP showed a 5.2-fold increase in renal hL-FABP mRNA compared to control Tg mice. When Tg animals received CP, hL-FABP mRNA increased 1.7-fold over that of control Tg animals at 24 h after CP exposure. It was much higher at 72 h, corresponding to an 81.1-fold increase over the level shown by the control Tg group. In CP-treated Tg mice that had been fed Bz, the increase in the renal transcription level of hL-FABP was 34.7-fold at 24 h and 88.3-fold at 72 h compared to control animals. These levels also corresponded to levels that were 6.6- and 16.9-fold higher at 24 and 72 h, respectively, than that of Bz-treated mice without CP. The renal hL-FABP transcription level in CP-treated Tg mice that had been fed Bz at 24 h after CP exposure was significantly increased to 21.3-fold over that of CP-treated Tg mice at 24 h. In brief, CP promoted the upregulation of renal hL-FABP transcription. Demonstrably, Bz promoted this upregulation not only in normal conditions but also in the CP-treated condition in earlier phases.

Effect of CP and fibrate on urinary shedding of hL-FABP

Bz was expected to increase the level of urinary hL-FABP in Tg mice. Admittedly, the urinary hL-FABP level of the Bz-treated Tg group ($n=7$) increased approximately eight-fold compared to control Tg animals ($n=7$; 102.0 ± 37.1 and 13.7 ± 5.6 μg per g urine creatinine, respectively, $P<0.05$; Figure 8). The CP-treated Tg mice at 24 h after CP exposure showed a greater than 100-fold increase of urinary hL-FABP excretion (1334.9 ± 220.3) compared to that of the serially collected timed-control specimens ($P<0.05$, $n=13$), and demonstrated a time-dependent increase (Figure 8; please note that the scale of the vertical bar is different between Figure 8a and b). In contrast, CP-treated Tg mice that had been fed Bz showed a maximum increase of urinary hL-FABP at 24 h (1548.4 ± 363.0) compared to the timed-control specimens ($n=12$); the level showed decreases at 48 and 72 h. In addition, CP-treated Tg mice fed with Bz showed significant attenuation of urinary hL-FABP compared to CP-treated Tg mice without Bz at the time point of 48 h (Bz + CP, 1525.5 ± 261.9; CP, 4726.1 ± 545.0, $P<0.05$) and 72 h (Bz + CP, 966.2 ± 242.6; CP, 8797.2 ± 1015.1, $P<0.05$).

Effect of CP and fibrate on plasma hL-FABP

The plasma hL-FABP level of Bz-treated Tg mice (Figure 9a) was 17-fold greater than that of control animals (99.9 ± 22.2 and 5.8 ± 2.0 ng ml^{-1}, respectively, $P<0.05$). Although the plasma hL-FABP level of both CP-treated Tg mice fed and not fed Bz increased in a time-dependent manner, the change in CP-treated Tg mice that had not been fed Bz was much greater: 24 h, 18.3 ± 11.9; 72 h, 133.6 ± 53.2. These levels corresponded, respectively, to 3.2- and 23-fold increases over the mean plasma level in the control Tg group (Figure 9b). However, minimal levels were found in CP-treated Tg mice that were fed Bz: 24 h, 120.7 ± 44.6; 72 h, 133.9 ± 34.2. These

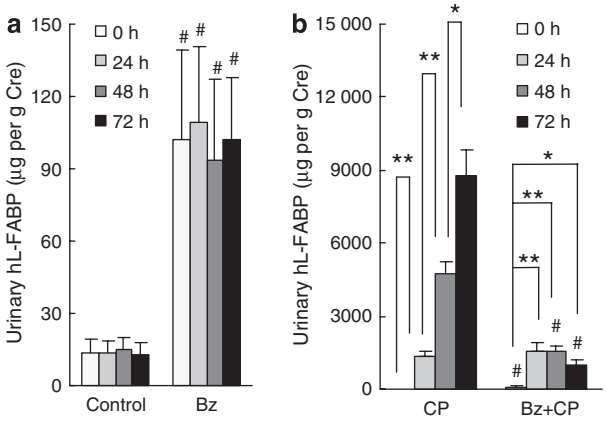

Figure 8 | Time course of urinary hL-FABP in Tg mice. (**a**) Time course of urinary hL-FABP in control and Bz groups. Statistically significant differences ($^{\#}P<0.05$) were indicated when the Bz group was compared to the control Tg group at the same time point. (**b**) Time course of urinary hL-FABP in CP-alone and Bz + CP groups. Both CP- and Bz + CP-treated mice displayed extremely high levels of urinary hL-FABP at 24 h after CP administration compared to those before CP administration. Although CP-treated mice showed a significant increase in the urinary hL-FABP level in a time-dependent manner, Bz + CP-treated mice showed a time-dependent decrease at 48 and 72 h. Statistically significant differences ($^{\#}P<0.05$) were indicated when the Bz + CP group was compared to the CP-treated Tg group at the same time point. Statistically significant differences ($^{*}P<0.05$, $^{**}P<0.01$) in serially sampled urine were indicated for the CP -alone and Bz + CP groups.

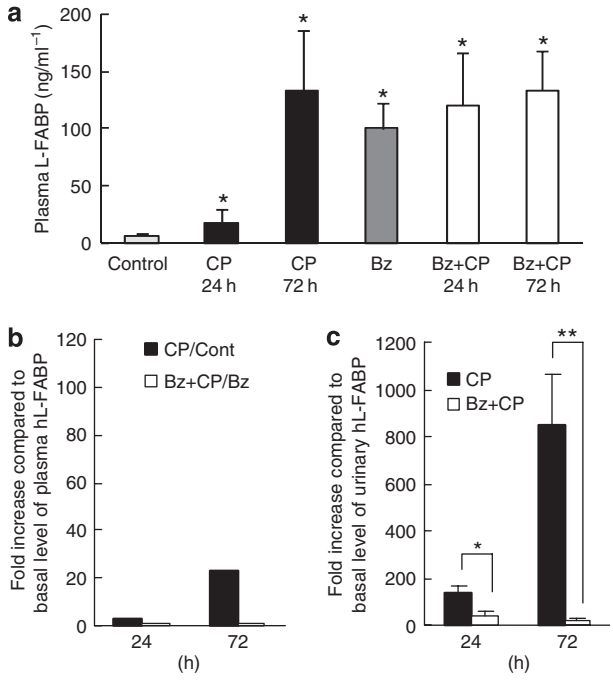

Figure 9 | Plasma hL-FABP levels and fold increase of plasma and urinary hL-FABP in Tg mice. (**a**) Plasma hL-FABP levels in Tg mice. Statistically significant differences ($^{*}P<0.05$) were indicated compared to the control Tg group. (**b**) Fold increase of plasma hL-FABP in Tg mice compared to the basal level. (**c**) Fold increase of urinary hL-FABP in Tg mice compared to the basal level. Statistically significant differences ($^{*}P<0.05$, $^{**}P<0.01$) were indicated when the Bz + CP group was compared to the CP-treated Tg group.

levels corresponded, respectively, to 1.2- and 1.3-fold increases compared to the mean plasma levels at those time points in Bz-treated Tg mice without CP. The fold increase of urinary hL-FABP shedding in serially sampled urine in CP-treated Tg mice without Bz was significantly larger compared to that of CP-treated Tg mice fed with Bz at 24 and 72 h after CP exposure (Figure 9c). The level was quite high as early as 24 h after CP exposure (CP, 139.2 ± 30.9; Bz + CP, 42.8 ± 15.0; $P < 0.05$) compared to the basal levels of serially sampled urine. The difference between fold increases of plasma and urinary hL-FABP was already apparent in an earlier phase of CP-AKI, where even BUN was equivalent to the basal level. Therefore, as a sensitive AKI biomarker, the monitoring of urinary hL-FABP was inferred to be clearly superior to monitoring plasma concentration. At the same time, urinary *N*-acetyl-β-D-glucosaminidase (NAG) levels in both CP-treated Tg mice fed and not fed Bz were not significantly changed through 72 h after CP administration, as compared to the basal level (44.9 ± 3.8 and 45.9 ± 4.4 U per g Cre, respectively). A recent study also suggested that urinary NAG was insensitive to detect CP-AKI within 72 h, at least in a mice model.[25]

Tubular accumulation of lipid and toxic lipid peroxidation products

Next, CP-induced disorder of lipid metabolism was examined in CP-treated kidneys. Sudan III staining was used for kidney sections at 72 h after CP administration, revealing numerous red lipid droplets in the cytoplasmic region of early segments of the proximal tubules in CP-treated WT (Figure 10a) and Tg (Figure 10b) kidney. In addition, lipid accumulation was rarely detected in kidneys of CP-treated Tg mice that had been fed Bz (Figure 10d), but not detected in CP-treated WT mice fed with Bz (Figure 10c). The staining was almost undetectable in the kidney obtained from control and Bz-treated mice without CP (data not shown). Glomeruli and medulla were negative for Sudan III staining.

Similarly, CP-treated WT mice, CP-treated Tg mice fed no Bz, and CP-treated WT mice fed Bz showed massive accumulation of 4-hydroxy-2-hexenal (HHE) in their kidneys: HHE, as well as 4-hydroxy-nonenal, is a highly toxic aldehyde generated during lipid peroxidation. We have recently reported the presence of HHE in AKI kidney, especially after ischemia–reperfusion injury;[26] HHE was again detected in CP-AKI kidney (Figure 11a). However, no such accumulation was observed in the kidneys of CP-treated Tg mice that had been fed Bz (Figure 11b). This finding supported that of western blot analysis derived from whole kidney lysate (Figure 11c). Localization of HHE was limited in damaged tubules in early segments of the proximal tubules. The hL-FABP-positive tubules were inferred to have been preserved and have escaped from HHE accumulation. Based on these results, pretreatment with Bz reduced CP-induced tubular accumulation of lipid and lipid peroxidation products almost completely through the upregulation of tubular L-FABP.

DISCUSSION

The results of this study show that CP at a dose of 20 mg kg^{-1} induced severe AKI, a result that was confirmed by measuring histological findings and ATN scoring; BUN increased greatly to around 150 mg per 100 ml in both WT and Tg mice by 72 h after CP injection. Moreover, histological deterioration of CP-induced AKI in WT was comparable to that of Tg.

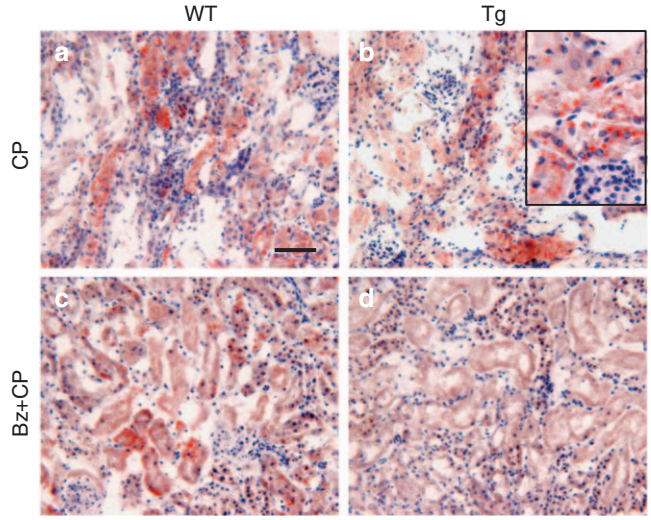

Figure 10 | Sudan III staining in kidney of CP-alone and Bz + CP-treated WT and Tg mice at 72 h after CP administration. Although tubular lipid accumulation of (**a**) CP-treated and (**c**) Bz + CP-treated WT and (**b**) CP-treated Tg mice at 72 h after CP administration was similarly prominent, (**d**) Bz + CP-treated Tg mice showed almost no droplet of lipid compared to those of other CP-treated animals (bar = 50 μm).

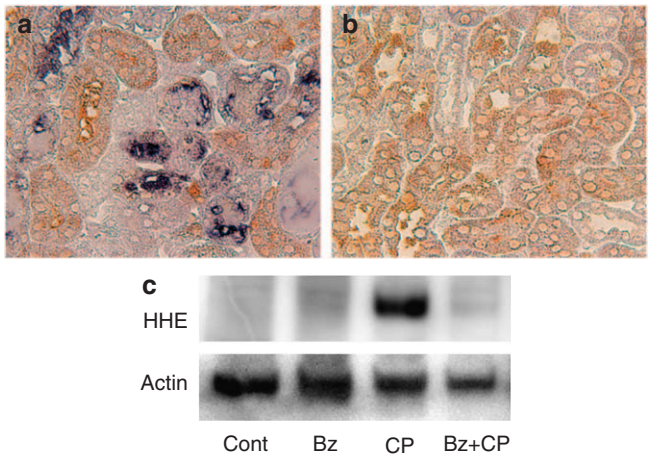

Figure 11 | Double immunohistochemical staining of HHE and hL-FABP in Tg mouse kidney and western blot analysis of HHE. Representative images showing stained HHE and hL-FABP in (**a**) CP-treated Tg kidney and (**b**) Bz + CP-treated Tg kidney. (**c**) Representative image of western blot analysis of HHE. CP-treated Tg mice exhibited severe accumulation of HHE in damaged tubules, whereas this accumulation was virtually absent in Bz + CP-treated kidney (bar = 50 μm). These findings were also verified using western blot analysis with whole kidney lysate.

Pretreatment with Bz in WT animals was not effective in reducing CP-induced AKI in terms of BUN and histological findings. Pretreatment with Bz in Tg animals was shown to ameliorate CP-induced AKI in this study. Yamamoto *et al.*[8] recently reported reduced susceptibility of ischemia–reperfusion injury in Tg mice compared to that of WT mice, in which renal hL-FABP expression played a pivotal role in the amelioration of AKI. Therefore, we believe that a sufficient amount of expression of renal hL-FABP is needed to ameliorate CP-mediated AKI.

The renal transcription level of L-FABP and protein expression in Tg mice treated with CP + Bz at 24 h after CP exposure were increased much more than those without Bz, although urinary L-FABP levels in those two groups were almost equivalent. Immunohistochemical analysis demonstrated cytosolic staining of hL-FABP in control animals. However, kidney tissue obtained from CP-treated Tg mice showed remarkable brush-border loss and lumen dilatation, and cytosolic immunoreactivity of hL-FABP had virtually disappeared. The Bz pretreatment showed its efficacy in improving those findings. Because CP inhibits genomic replication via its binding to a DNA double strand, the transcription level of hL-FABP will be affected by CP. The initial shedding of urinary hL-FABP in CP-AKI will be dependent on proximal tubular cytosolic protein, as recently discussed in ischemia–reperfusion injury.[8] In ischemia–reperfusion, the transcription level was higher 15 h later. The recovery of transcription level is necessary for reduction of renal injury in CP-AKI, and pretreatment using Bz is valuable. The cytosolic depletion of hL-FABP seen in CP-treated kidney of Tg mice presumably degrades tubular viability and promotes apoptosis based on the malfunction in handling the lipid metabolism and coping with lipid peroxidation, as presented in this study. Proximal tubular cells might overcome CP-AKI through preservation of the balance between cytosolic L-FABP as a fatty acid transporter and a toxic lipid peroxidation product such as HHE.

Recently, we have confirmed that increased shedding of urinary L-FABP is an early biomarker of AKI not only in the CP model of AKI in mice but also during ischemia–reperfusion in patients undergoing cardiac surgery.[27] The rapid translocation of hL-FABP to the nuclear compartment is likely related to a post-translational modification of L-FABP and induced by CP. Admittedly, despite the massive translocation of L-FABP into the urine in the early phase of CP-AKI and the significant attenuation of renal dysfunction and morphological damage, the Bz-mediated renal upregulation of L-FABP was approximately 1.5-fold in CP-treated Tg kidneys with Bz, compared to those without Bz, when kidneys were obtained 24 h later. Further studies are needed to understand the mechanism(s) of increased shedding of renal hL-FABP during proximal tubular injury.

In a previous study, Portilla and co-workers reported that the inhibition of peroxisomal and mitochondrial fatty acid oxidation observed in kidney tissue of mice undergoing ischemia–reperfusion AKI and CP-induced AKI results from the reduced activity of PPAR.[12–14,28–33] The results of this study support these findings because the renal upregulation of hL-FABP mRNA by Bz only showed efficacy in ameliorating CP-AKI in Tg mice. As a matter of fact, the peroxisome proliferator response element exists in the promoter region of hL-FABP; it therefore played a crucial role in fatty acid oxidation in the proximal tubules. Because CP is an antitumor drug and the lethal dosage was administered in this study, the toxic effects of CP aside from nephrotoxicity might affect the urine level of hL-FABP in CP-AKI. Increased circulating L-FABP mediated by Bz might also increase megalin-mediated endocytosis of L-FABP from the urine space after filtration.[34–37] It is plausible that enhancement of cytosolic L-FABP expression in the proximal tubules was derived not only from itself but also from increased filtration of circulating L-FABP, which contributed to amelioration of CP-induced AKI. In this study, the plasma level of hL-FABP was increased to a significant level at 24 h after CP administration, and it increased further until 72 h. The basal level of plasma L-FABP had already increased compared to that without Bz when animals were pretreated with Bz. Moreover, CP administration increased plasma hL-FABP but not to a significant level. It remained at that same level until 72 h.

We next standardized the level of increase by the basal level of control or Bz, and expressed it as a fold increase, as presented in Figure 9. Compared to the fold increase in plasma hL-FABP at 24 h, the fold increase of urine hL-FABP at 24 h in CP was enormous: 3.2-fold in plasma versus 139-fold in urine. The fold increases at 24 h were 1.2-fold in plasma (Figure 9b) and 43-fold in urine (Figure 9c) when animals were pretreated with Bz. Because the L-FABP coding gene has peroxisome proliferator response element in its promoter region, as described above, the pretreatment using a PPAR ligand such as Bz potentially elevated plasma L-FABP through the liver, intestine, and renal upregulation of L-FABP transcription in Tg mice. The significant increase of plasma L-FABP that was found for CP-treated Tg mice between 24 and 72 h might be influenced not only by the CP-induced renal upregulation of L-FABP but also by the decrease of the glomerular filtration rate and/or tubular reabsorption capabilities. However, it is noteworthy that the increased levels of urinary L-FABP 24 h later in CP-treated Tg mice fed and not fed Bz were very much larger than those of plasma L-FABP at the same time point. In addition, C57BL/6 WT mice pretreated with Bz showed no improvement in renal function, morphological damage, or lipid accumulation induced by CP, even though it was thought to increase circulating mouse L-FABP derived from the liver and/or intestine. Consequently, at least in the AKI model used in this study, the urinary hL-FABP level in Tg mice is seemingly not parallel to the circulating plasma hL-FABP level, and is rather defined by the transcription level of the renal proximal tubules.

Based on these data, the efficacy of urine hL-FABP as a biomarker of CP-AKI is readily apparent because the increase

of urine hL-FABP was earlier than that of BUN. In fact, BUN at 24 h after CP injection remained around 25 mg kg^{-1} in both WT and Tg animals. At the 24 h time point, it was difficult to foretell the huge increase of BUN seen at 72 h and later, but urine L-FABP increased remarkably by 24 h after CP injection. Urine L-FABP was increased within the first 2 h after CP administration (data not shown).

The hL-FABP Tg mice are also sensitive to a wide variety of AKI such as ischemia–reperfusion,[8] radio-contrast media,[38] cyclooxygenase-2 inhibitors,[39] and aminoglycosides (unpublished data). For this reason, these 'humanized' mice are presumably useful for purposes of nephrotoxicity validation during drug development.

In summary, CP-AKI was ameliorated by the PPAR agonist Bz in Tg mice. This efficacy was, in part, mediated by increased renal expression of L-FABP. Reduction of lipotoxicity and apoptosis in renal tubules contributed to that amelioration. Urine L-FABP was an earlier indicator of CP-AKI when compared to BUN and thus proved itself to be a useful early biomarker for the detection of drug-induced nephrotoxicity.

MATERIALS AND METHODS

Animals

The engineering of hL-FABP chromosomal Tg mice is detailed elsewhere.[8] This Tg mice strain is not forcibly overexpressing. Briefly, the genomic DNA of hL-FABP, including its promoter region (13 kb), was microinjected into fertilized eggs obtained from C57BL/6 and CBA mice; ICR mice were used as transfected egg recipients. The resultant Tg mice were backcrossed for more than nine generations onto C57BL/6 mice to obtain congenic mutant mice on an inbred background. Only heterozygous L-FABP Tg mice were used in this experiment. Male WT and L-FABP Tg mice weighing 25–35 g were allowed food and water *ad libitum*.

Experimental model

Male WT and hL-FABP Tg mice were divided at random into four groups, kept in glass-shielded metabolic cages (Metabolica; Sugiyamagen, Tokyo, Japan), and fed with a standard chow diet or with a special diet containing Bz (0.5% wt/wt, generously provided by Kissei Pharmaceutical Co. Ltd, Matsumoto, Japan) for 7 days before the induction of acute renal failure. CP (generously provided by Nippon Kayaku Co. Ltd, Tokyo, Japan) or saline was administered using a single intraperitoneal injection of 20 mg per kg body weight. Immediately before and after injection of CP, blood and urine were serially collected at each 24 h interval. Mice were killed at 72 h after intraperitoneal injection, and kidneys were harvested for reverse transcriptase-PCR, western blot analysis, and immunohistological analysis. In a separate procedure, Tg kidney specimens were similarly collected at 24 h after CP injection.

All experiments were conducted in accordance with the NIH Guide for the Care and Use of Laboratory Animals (US Department of Health and Human Services, Public Health Services, National Institutes of Health, NIH publication no. 86-23, 1985).

Measurement of BUN

BUN was measured by the urease–indophenol method with Urea NB (Wako Pure Chemical Industries Ltd, Osaka, Japan), using an absorbance 96-well plate reader (SpectraMAX Plus; Molecular Devices Corp., Sunnyvale, CA, USA) at a wavelength of 570 nm.

Measurement of urinary creatinine

Urinary creatinine was measured using the colorimetric method based on hydrogen peroxide measurement (Nescoat VLII CRE; Alfresa Pharma Corp., Osaka, Japan), using the absorbance 96-well plate reader (Molecular Devices Corp.) loaded with a 546 and 660 nm filter.

Measurement of NAG

Urinary NAG was measured using a test (NAG Rate Test Shionogi; Shionogi & Co. Ltd, Osaka, Japan) that applied the colorimetric method based on free chlorophenol red measurement by hydrolysis, by which NAG reacts as sodio-3,3′-dichlorophenol-sulfonphthaleinyl NAG, using the absorbance 96-well plate reader (Molecular Devices Corp.) with a 575 nm filter.

Measurement of urinary and plasma hL-FABP by enzyme-linked immunosorbent assay

Urinary hL-FABP was measured using a sandwich enzyme-linked immunosorbent assay kit (CMIC Co. Ltd, Tokyo, Japan) following the manufacturer's protocol. The coefficient of variation for the obtained value was within 10% when intra-assay reproducibility was determined using the same sample eight times. The measurable range of this kit is 4–400 ng ml^{-1}. This assay system does not detect rodents' L-FABP, particularly that derived from WT mice. Urinary hL-FABP was expressed as the ratio of the urinary L-FABP in micrograms to the urinary creatinine.

Morphologic evaluation of kidneys

Formalin-fixed sections were stained with hematoxylin–eosin and periodic acid-Schiff. Morphological evaluation was performed using well-established criteria as the ATN score in a blind manner.

Immunohistochemical analyses

Immunohistochemical staining of 2 μm paraffin sections was performed using an indirect immunohistochemical technique. After deparaffinization, the nonspecific reaction for horseradish peroxidase was blocked using 3% hydrogen peroxide in methyl alcohol for 5 min.

Specimens were blocked initially using the mouse IgG blocking reagent (MOM; Vector Laboratories Inc., Burlingame, CA, USA) for immunohistochemical staining with mice monoclonal antibodies and by using rabbit IgG (DakoCytomation, Glostrup, Denmark) for rabbit polyclonal antibody. A primary monoclonal antibody of hL-FABP, which is not cross-reacting to mouse L-FABP, was applied to sections with 1:500 dilution and incubated for 1 h at room temperature. A primary polyclonal rabbit anti-ssDNA antibody (DakoCytomation) or monoclonal anti-HHE antibody (NOF Corp., Tokyo, Japan) with 1:100 dilutions was applied to sections and incubated for 2 h at room temperature. The subsequent procedure of sections was followed using a Vectorstain ABC system (Vector Laboratories Inc.), according to the manufacturer's protocol. For the substrate–chromogen reaction, diaminobenzidine tetrahydrochloride (Simple Stain DAB; Nichiei, Tokyo, Japan) was used, according to the manufacturer's protocol. Control sections were subjected to secondary antibody only (blank).

The antigen retrieval procedure by microwave was necessary for double staining with hL-FABP and HHE. The colorimetric detection

of HHE antibody was conducted using a combination of anti-mouse IgG-AP secondary antibody (F Hoffman-La Roche Ltd/Roche, Basel, Switzerland), nitro blue tetrazolium chloride/5-bromo-4-chloro-3-indolyl phosphate, and toluidine salt solution (Roche). These sections were counterstained by methyl green (Vector Laboratories Inc.). Immunohistochemical examinations were made using light microscopy (E600; Nikon Corp., Tokyo, Japan). Images were captured using a CCD camera (DXM1200; Nikon Corp.).

The level of tubular apoptosis was quantitated using the average number of ssDNA-positive cells per field. The number of ssDNA-positive tubular epithelial cells was determined in 10 randomly selected non-overlapping fields at $\times 200$ magnification in each section of the individual mouse renal cortex. The scores of respective kidneys were averaged, and the scores of each group were further averaged.

Sudan III staining was applied for renal lipid accumulation. Cryostat-frozen kidney sections of 10 μm were washed in 60% ethanol and incubated in Sudan III (Chroma-Gesellschaft Schmid GmbH and Co., Koengen, Germany) solution saturated with 70% ethanol at 37 °C for 1 h. After washing in 60% ethanol, these sections were counterstained with Mayer's hematoxylin (Vector Laboratories Inc.).

Quantitative real-time reverse transcriptase-PCR analysis

Total RNA was extracted from the whole kidney homogenates using Trizol (Invitrogen Corp., Carlsbad, CA, USA). QuantiTect Reverse Transcription Kit (Qiagen Inc., Hilden, Germany) was used according to the manufacturer's protocol to synthesize cDNA from total RNA. Renal transcription levels were assessed using real-time quantitative PCR (real-time PCR) with TaqMan Universal PCR Master Mix (Applied Biosystems, Foster City, CA, USA) and a PCR system (Prism 7000; Applied Biosystems), according to the manufacturer's instructions. The respective PCR primers were obtained (Assay-on-Demand; Applied Biosystems) as follows: hL-FABP (assay ID: Hs00155026_m1) and 18S ribosomal RNA (assay ID: Hs99999901_s1).

Western blot analysis

Harvested kidneys were homogenized on ice in a radioimmunoprecipitation assay buffer with protease inhibitors. The lysates were separated on a 10–20% gradient sodium dodecyl sulfate-polyacrylamide gel electrophoresis. After transferring proteins from the gel to a polyvinylidene difluoride membrane (Amersham Biosciences Corp., Uppsala, Sweden), western blot analysis was performed using 1:10 diluted horseradish peroxidase-labeled hL-FABP antibody or 1:500 diluted HHE antibody for 1 h at room temperature. Can Get Signal (Toyobo Co. Ltd, Osaka, Japan) was used in antibody dilution buffer to reduce the background level. Subsequently, the chemiluminescent signal labeled using ECL Plus (Amersham Biosciences Corp.) was detected using a CCD camera system (LAS-4000mini; Fuji Photo Film Co. Ltd, Tokyo, Japan). The membrane was then incubated at 50 °C for 30 min in a stripping buffer to remove all probes. The reprobing procedure was further performed with the antibody to actin (Chemicon Co. Ltd, Temecula, CA, USA).

Statistical analysis

The results of statistical analyses are expressed as means ± s.e.m.; $P<0.05$ was considered significant. Differences among groups at the same time point were examined using the Tukey–Kramer honestly significant difference test. Differences among experimental groups at different time points were confirmed using one-way analysis of variance followed by the Tukey–Kramer honestly significant difference test for individual comparison of group means. Differences among experimental groups in serial sampling results were compared using multiple analyses of variance, with calculations performed using software (JMP5.1.1; SAS Institute Inc., Cary, NC, USA).

ACKNOWLEDGMENTS

We are very grateful to Mrs Haba, Mrs Amitani, and Mr Onimaru, who assisted us with their technical support. Part of this study was supported by Health and Labor Sciences Research Grants for Research on the Human Genome, grants for Tissue Engineering Food Biotechnology (Grant no. 057100000661) from MHLW of Japan (EN and TS), funding from the BioBank Japan Project on the Implementation of Personalized Medicine (Grant no. 3023168), MEXT, Japan (EN), by the Special Coordination Funds for Promoting Science and Technologies (Grant no. 1200015), MEXT, Japan (EN), and by NIH/NIDDK RO1-DK075976 and a VA Merit Award, USA (DP).

REFERENCES

1. Chmurzynska A. The multigene family of fatty acid-binding proteins (FABPs): function, structure and polymorphism. *J Appl Genet* 2006; **47**: 39–48.
2. Haunerland NH, Spener F. Fatty acid-binding proteins—insights from genetic manipulations. *Prog Lipid Res* 2004; **43**: 328–349.
3. Kliewer SA, Forman BM, Blumberg B *et al.* Differential expression and activation of a family of murine peroxisome proliferator-activated receptors. *Proc Natl Acad Sci USA* 1994; **91**: 7355–7359.
4. Zimmerman AW, Veerkamp JH. New insights into the structure and function of fatty acid-binding proteins. *Cell Mol Life Sci* 2002; **59**: 1096–1116.
5. Antonenkov VD, Sormunen RT, Ohlmeier S *et al.* Localization of a portion of the liver isoform of fatty-acid-binding protein (L-FABP) to peroxisomes. *Biochem J* 2006; **394**: 475–484.
6. Bennaars-Eiden A, Higgins L, Hertzel AV *et al.* Covalent modification of epithelial fatty acid-binding protein by 4-hydroxynonenal *in vitro* and *in vivo*. Evidence for a role in antioxidant biology. *J Biol Chem* 2002; **277**: 50693–50702.
7. Wang G, Gong Y, Anderson J *et al.* Antioxidative function of L-FABP in L-FABP stably transfected Chang liver cells. *Hepatology* 2005; **42**: 871–879.
8. Yamamoto T, Noiri E, Ono Y *et al.* Renal L-type fatty acid binding protein in acute ischemic injury. *J Am Soc Nephrol* 2007; **18**: 2894–2902.
9. Oyama Y, Takeda T, Hama H *et al.* Evidence for megalin-mediated proximal tubular uptake of L-FABP, a carrier of potentially nephrotoxic molecules. *Lab Invest* 2005; **85**: 522–531.
10. Hishikawa K, Marumo T, Miura S *et al.* Musculin/MyoR is expressed in kidney side population cells and can regulate their function. *J Cell Biol* 2005; **169**: 921–928.
11. Yang T, Michele DE, Park J *et al.* Expression of peroxisomal proliferator-activated receptors and retinoid X receptors in the kidney. *Am J Physiol* 1999; **277**: F966–F973.
12. Li S, Basnakian A, Bhatt R *et al.* PPAR-alpha ligand ameliorates acute renal failure by reducing cisplatin-induced increased expression of renal endonuclease G. *Am J Physiol Renal Physiol* 2004; **287**: F990–F998.
13. Li S, Gokden N, Okusa MD *et al.* Anti-inflammatory effect of fibrate protects from cisplatin-induced ARF. *Am J Physiol Renal Physiol* 2005; **289**: F469–F480.
14. Li S, Wu P, Yarlagadda P *et al.* PPAR alpha ligand protects during cisplatin-induced acute renal failure by preventing inhibition of renal FAO and PDC activity. *Am J Physiol Renal Physiol* 2004; **286**: F572–F580.
15. Negishi K, Noiri E, Sugaya T *et al.* A role of liver fatty acid-binding protein in cisplatin-induced acute renal failure. *Kidney Int* 2007; **72**: 348–358.
16. Simon TC, Roth KA, Gordon JI. Use of transgenic mice to map *cis*-acting elements in the liver fatty acid-binding protein gene (Fabpl) that regulate its cell lineage-specific, differentiation-dependent, and spatial patterns of expression in the gut epithelium and in the liver acinus. *J Biol Chem* 1993; **268**: 18345–18358.
17. Sweetser DA, Lowe JB, Gordon JI. The nucleotide sequence of the rat liver fatty acid-binding protein gene. Evidence that exon 1 encodes an oligopeptide domain shared by a family of proteins which bind hydrophobic ligands. *J Biol Chem* 1986; **261**: 5553–5561.

18. Kamijo A, Kimura K, Sugaya T *et al.* Urinary fatty acid-binding protein as a new clinical marker of the progression of chronic renal disease. *J Lab Clin Med* 2004; **143**: 23–30.
19. Kamijo A, Sugaya T, Hikawa A *et al.* Urinary excretion of fatty acid-binding protein reflects stress overload on the proximal tubules. *Am J Pathol* 2004; **165**: 1243–1255.
20. Kamijo-Ikemori A, Sugaya T, Obama A *et al.* Liver-type fatty acid-binding protein attenuates renal injury induced by unilateral ureteral obstruction. *Am J Pathol* 2006; **169**: 1107–1117.
21. Solez K, Morel-Maroger L, Sraer JD. The morphology of 'acute tubular necrosis' in man: analysis of 57 renal biopsies and a comparison with the glycerol model. *Medicine (Baltimore)* 1979; **58**: 362–376.
22. Noiri E, Peresleni T, Miller F *et al. In vivo* targeting of inducible NO synthase with oligodeoxynucleotides protects rat kidney against ischemia. *J Clin Invest* 1996; **97**: 2377–2383.
23. Kawarada Y, Miura N, Sugiyama T. Antibody against single-stranded DNA useful for detecting apoptotic cells recognizes hexadeoxynucleotides with various base sequences. *J Biochem (Tokyo)* 1998; **123**: 492–498.
24. Naruse I, Keino H, Kawarada Y. Antibody against single-stranded DNA detects both programmed cell death and drug-induced apoptosis. *Histochemistry* 1994; **101**: 73–78.
25. Mishra J, Mori K, Ma Q *et al.* Neutrophil gelatinase-associated lipocalin: a novel early urinary biomarker for cisplatin nephrotoxicity. *Am J Nephrol* 2004; **24**: 307–315.
26. Doi K, Suzuki Y, Nakao A *et al.* Radical scavenger edaravone developed for clinical use ameliorates ischemia/reperfusion injury in rat kidney. *Kidney Int* 2004; **65**: 1714–1723.
27. Portilla D, Dent C, Sugaya T *et al.* Liver fatty acid-binding protein as a biomarker of acute kidney injury after cardiac surgery. *Kidney Int* 2008; **73**: 465-472.
28. Portilla D. Role of fatty acid beta-oxidation and calcium-independent phospholipase A2 in ischemic acute renal failure. *Curr Opin Nephrol Hypertens* 1999; **8**: 473–477.
29. Portilla D. Energy metabolism and cytotoxicity. *Semin Nephrol* 2003; **23**: 432–438.
30. Portilla D, Dai G, Peters JM *et al.* Etomoxir-induced PPARalpha-modulated enzymes protect during acute renal failure. *Am J Physiol Renal Physiol* 2000; **278**: F667–F675.
31. Nagothu KK, Bhatt R, Kaushal GP *et al.* Fibrate prevents cisplatin-induced proximal tubule cell death. *Kidney Int* 2005; **68**: 2680–2693.
32. Portilla D, Dai G, McClure T *et al.* Alterations of PPARalpha and its coactivator PGC-1 in cisplatin-induced acute renal failure. *Kidney Int* 2002; **62**: 1208–1218.
33. Portilla D, Li S, Nagothu KK *et al.* Metabolomic study of cisplatin-induced nephrotoxicity. *Kidney Int* 2006; **69**: 2194–2204.
34. Christensen EI, Birn H. Megalin and cubilin: synergistic endocytic receptors in renal proximal tubule. *Am J Physiol Renal Physiol* 2001; **280**: F562–F573.
35. Kozyraki R, Fyfe J, Verroust PJ *et al.* Megalin-dependent cubilin-mediated endocytosis is a major pathway for the apical uptake of transferrin in polarized epithelia. *Proc Natl Acad Sci USA* 2001; **98**: 12491–12496.
36. Moestrup SK, Verroust PJ. Megalin- and cubilin-mediated endocytosis of protein-bound vitamins, lipids, and hormones in polarized epithelia. *Annu Rev Nutr* 2001; **21**: 407–428.
37. Zou Z, Chung B, Nguyen T *et al.* Linking receptor-mediated endocytosis and cell signaling: evidence for regulated intramembrane proteolysis of megalin in proximal tubule. *J Biol Chem* 2004; **279**: 34302–34310.
38. Nakamura T, Sugaya T, Node K *et al.* Urinary excretion of liver-type fatty acid-binding protein in contrast medium-induced nephropathy. *Am J Kidney Dis* 2006; **47**: 439–444.
39. Tanaka T, Noiri E, Yamamoto T *et al.* Urine human L-FABP is a potential biomarker to predict COX-inhibitor induced renal injury. *Nephron Exp Nephrol* 2008; **108**: e19–e26.